BEHAVIOR OF REINFORCED CONCRETE BEAM-COLUMN-SLAB SUBASSEMBLAGES SUBJECTED TO BI-DIRECTIONAL LOAD REVERSALS

Kazuhiro KITAYAMA[1], and Shunsuke OTANI[2]

[1]Department of Architecture, Utsunomiya University, Utsunomiya-shi, Tochigi, Japan
[2]Department of Architecture, University of Tokyo, Bunkyo-ku, Tokyo, Japan

SUMMARY

Two interior and one exterior beam-column-slab subassemblages were tested under bi-directional reversed cyclic loading. Beam-column connection of all specimens did not fail in shear despite of the high shear stress input to the connection. The confinement to the joint core concrete by the transverse beams and slabs prevented the joint shear failure. The pinching behavior was caused by the existence of slabs in spite of the improvement in the bond along beam bars within the connection. For an exterior joint specimen, the entire slab width is regarded as effective if the transverse beams do not fail in torsion.

INTRODUCTION

The hysteretic behavior of a beam-column connection is influenced by the bond characteristics along beam bars within the connection. An improvement in the bond characteristics makes it possible to develop a good spindle-shape hysteresis with flexural yielding at the critical region at beam ends (Refs.1,2). On the other hand, the bond deterioration yields a pinching hysteresis loop attributable to the pull-out of the beam bars from the connection, and also changes the shear resisting mechanism in the connection to cause shear failure at a large deformation (Refs.2,3).

In the past, most of beam-column sub-assemblage tests were carried out on plane beam-column connections, loaded in one horizontal direction. The beam-column connection in an actual structure has both slabs and transverse beams and is subjected to bi-directional loading under earthquake motions. Therefore, it was decided that three-dimensional beam-column connections with slabs be tested under the bi-directional loading. The main variable in the test was chosen to be the bond conditions along the beam bars within the connection.

EXPERIMENTAL PROGRAM

Specimens Three half-scale reinforced concrete three-dimensional beam-column connections with slabs (called K-series) were tested; two interior connections with four beams connected in the orthogonal directions (Specimens K1 and K2) and one exterior connection with three beams connected in the orthogonal directions (Specimen K3). The column dimensions were varied in the two interior connections; i.e., 275x275 mm in Specimen K1 and 375x375 mm in Specimen K2. The column dimensions in Specimen K3 were the same as that in Specimen K1. The beam dimensions were common in the three specimens; 200x300 mm for the longitudinal beams (in the primary loading direction) and 200x285 mm for the transverse beams. The thickness of slabs was 70 mm. The four corners of the square slab were

trimmed to fit into the testing apparatus.

Reinforcement details of the specimens are shown in Fig.1. Beam bars of the interior beams passed through the connections, whereas the top and bottom beam bars of the exterior beam were anchored within the connection. D13 bars were used as the column reinforcement in the three specimens. The size of the beam bars was varied in the two interior specimens; D13 bars in Specimen K1 and D10 bars in Specimen K2. D10 bars were used as the beam reinforcement in Specimen K3. A nominal amount of lateral reinforcement (D6 bars at 50 mm on centers in Specimens K1 and K2 , at 55 mm on centers in Specimen K3) was provided within the connection, the same as the amount of shear reinforcement required in the middle part of the column in accordance with the AIJ Standard (Ref.4). The slab was reinforced with D6 bars at 180 mm on centers in a single layer, with a 180^{o} hook at each end, but the slab bars in Specimen K3 parallel to the longitudinal beam were anchored in the transverse beams with 90^{o} hooks.

The bond conditions of beam bars was made significantly different in the two interior connection specimens by varying the column width to the beam bar diameter ratio. The bond index is defined as an average bond stress of a beam bar within the connection under simultaneous tensile and compressive yielding assumed at the column faces (Ref.1);

$$u_b = f_y \, (d_b/h_c) \, / \, 2$$

where f_y : yield strength of a beam bar, d_b : diameter of a beam bar and h_c : column width. The index values are 102 kgf/cm^2 (10.0 MPa) for Specimen K1 and 57 kgf/cm^2 (5.6 MPa) for Specimen K2 using the actual yield strength of the beam bar. From these index values, the bond of beam bars in Specimen K1 was expected to be quite severe compared to Specimen K2.

The concrete was cast in the upright position in two stages; i.e., the concrete was first placed to the top of the slab, and then cast in the upper column after a day.

Material Properties The compressive strength of the first batch of the concrete was 244 kgf/cm^2 (23.9 MPa) for Specimens K1 and K2, and 199 kgf/cm^2 (19.5 MPa) for Specimen K3. The compressive strength of the second batch was 266 kgf/cm^2 (26.1 MPa) for Specimens K1 and K2, and 196 kgf/cm^2 (19.2 MPa) for Specimen K3.

The yield strength was 4,420 kgf/cm^2 (433 MPa) for the D13 bars, 4,460 kgf/cm^2 (437 MPa) for the D10 bars, and 4,010 kgf/cm^2 (393 MPa) for the D6 bars at 0.2 % offset.

Testing Method The loading apparatus is shown in Fig.2. The specimens were tested in the upright position. The base of the specimen was supported by a universal joint. The free ends of the beams were supported by vertical rigid members equipped with universal joints at their ends, creating roller support conditions in the horizontal plane.

The distance from the column center to the beam-end support was 1,350 mm, and the distance from the beam center to the bottom support or to the top horizontal loading point was 735 mm.

The constant vertical load (an average axial stress of 20 kgf/cm^2 or 2.0 MPa) and reversing bi-directional horizontal loads were applied at the top of the column through the tri-directional joint by three actuators. Counter-weights balanced the weight of the horizontal actuators. A set of

pantograph, parallel to the longitudinal beam, prevented a specimen from rotating around the vertical axis.

The deflections of beams and columns relative to the beam-column connection, axial deformation at the top and bottom fiber of beams, beam axial deformation, rotations of beam-end support points around beam axes and connection shear deformation were measured by strain-gauge type displacement transducers. The strain distribution of beam longitudinal reinforcement within and immediately outside the beam-column connection and that of slab reinforcement, the strain of lateral reinforcement within a connection and that of column reinforcement at the critical section were measured by strain gauges. The loads applied by the actuators and beam-end support reactions were measured by load cells.

Loading History In first two cycles, specimens were loaded in a longitudinal direction up to the half of an ultimate capacity calculated. Subsequently the yield story drift ($_{y}$) was determined and the bi-directional story drift two and four times as large as the yield story drift as shown in Fig.3 was forced. If four times the yield story drift angle was larger than 1/50 rad, the applied story drift history was displaced by the story drift angle of 1/50 rad instead of four times the yield one.

TEST RESULTS

Three specimens developed flexural yielding at the beam ends and the connections did not fail in shear, nor did the transverse beams (edge beams) of Specimen K3 in torsion induced by the tensile forces of the slab reinforcement.

The column reinforcement of each specimens was observed to yield at a story drift angle as follows; 1/139 rad (cycle 3) during the uni-directional loading when the beam reinforcement started to yield in Specimen K1, 1/108 rad (cycle 7) during the bi-directional loading after the beam yielding in Specimen K2 and 1/69 rad (cycle 8) during the bi-directional loading after the beam yielding in Specimen K3.

Crack Patterns The crack patterns of three specimens observed at the end of loading are shown in Fig.4. Specimen K1 developed a single and wide concentrated crack at the critical section of the beams and developed hardly any additional cracks in the beams after a story drift angle of 1/50 rad. The shell concrete spalled in the four corners near and within the connection at a story drift angle of 1/25 rad.

On the contrary, Specimen K2 developed fine flexural cracks along the beams after a story drift angle of 1/54 rad. As expected, the bond characteristics along the beam bars were significantly improved in the connection of Specimen K2 from Specimen K1. Cracks were observed more closely in the slab partially because the beams had to deform more in Specimen K2 because the column was stiff.

For Specimen K3, torsional cracks were observed in the transverse beams near the column during the loading in the longitudinal direction. But the width was small and the transverse beams did not fail in torsion. Diagonal shear cracks were observed in the connection panel region in the transverse direction. During loading in the transverse direction, cracks in the slab ran almost parallel to the longitudinal beam and did not incline toward the slab corner as seen during loading in the longitudinal

direction.

Hysteretic Characteristics The story shear-story drift relations in the longitudinal direction are shown in Fig.5. The story drift at yielding was 10.6 mm for Specimen K1 and 6.8 mm for Specimen K2, the difference of which was attributable to the stiffness of the columns.

A story shear resistance in a direction could be reduced during the loading in the orthogonal direction although the displacement was maintained in the direction, the phenomenon of which is called the biaxial interaction of resistances. In other words, the resistance in one direction is influenced by the deflections in the orthogonal direction. Such phenomenon could be observed between points A and B in Fig.5. Because of the biaxial interaction, the apparent area of a hysteresis loop increases if the load is applied in a manner described in this paper.

Specimens K1 and K2 showed a pinching hysteresis shape under cyclic load reversals. The equivalent viscous damping ratio is used to quantify the fatness of hysteresis loops. The equivalent viscous damping ratio of Specimens K1 and K2 were 0.07 and 0.12 respectively at the story drift angle of approximately 1/50 rad. This means that the hysteresis loop in Specimen K2 was fatter than that in Specimen K1.

The behavior of a three-dimensional beam-column connection and a plane connection is compared using the specimens with comparable bond index values and subjected to comparable loading. The bond index value was 57 kgf/cm^2 (5.6 MPa) for Specimen K2, and 52 kgf/cm^2 (5.1 MPa) for Specimen C2 (a plane beam-column connection specimen tested previously, Ref.1). The equivalent viscous damping ratio was 0.12 for Specimen K2 at a cumulative ductility factor of 35.5 (in the second cycle at a story drift angle of 1/54 rad), and 0.21 for Specimen C2 at a cumulative ductility factor of 37.0 (in the fifth cycle at a story drift angle of 1/46 rad). Accordingly, the equivalent viscous damping ratio was considerably smaller in Specimen K2 at a comparable story drift angle and cumulative ductility factor. It is likely that the slab might contribute to the pinching in the shape of hysteretic loops.

Generally, such pinching hysteresis shape is observed without bar slip and shear failure when the amount of reinforcement differs significantly at the top and bottom of a beam section. The area of the top beam bars was twice the bottom bars in Specimen C2, although the specimen showed a nice spindle shape hysteresis. In the test of Specimen K2, ten slab bars were observed to have yielded and the remaining two slab bars reached strains above 0.1 % at a story drift angle of 1/54 rad. Therefore, eleven slab bars may well be assumed effective on the beam resistance. Consequently, the total steel area (= 851 mm^2) of the top beam bars became 2.4 times that of bottom beam bars(= 357 mm^2), the ratio which is not much different from that of specimen C2. Therefore, the difference in the amount of the top and bottom reinforcement does not describe the pinching phenomenon of the three dimensional subassemblage.

The stress distribution in the beam top and bottom reinforcement of Specimen K2 are shown in Fig.6 at a story drift angle of 1/216 rad. The stress was calculated from the strain using the Ramberg-Osgood model for the stress-strain relationship of the steel. A solid line represents the distribution during the loading in the positive direction and a broken line in the negative direction. When the bottom beam bar yielded in tension at an end of a connection, the stress at the other end remained in compression, indicating a good bond characteristics of the beam bottom

reinforcement within the connection.

On the contrary, the stress along the beam top bar remained in tension over the entire width of the connection. The stress distributed in a V-shape with a minimum stress appearing near the center. Such stress distribution could not be caused by the bond deterioration. It was thought that the location of the neutral axis rised above the beam top reinforcement under positive bending (beam bottom fiber in tension) to yield a tensile stress in the beam top reinforcement at the section. Therefore, the entire beam top reinforcement within the connection developed tensile stresses. At the same time, the crack at the beam bottom must open wide to satisfy the compatibility of strains in the section. Hence, the closing of the flexural crack at the beam critical section was delayed when the load was reversed, causing the pinching behavior in Specimen K2.

Displacement Contribution The contribution of parts of Specimens K1 and K2 to the story drift was estimated and shown in Fig.7. The contribution of parts of Specimen K3 for a transverse direction was similar to that of Specimen K1. The contribution of the beam-column connection panel deformation was calculated as the total deflection less the contribution from the beam and column deflections. Note that the beam deformation included a deformation caused by the pull-out of the beam reinforcement from the connection. An abrupt increase in this ratio generally identifies the mode of failure corresponding to the deformation.

The ratio of the connection deformation in the three specimens remained almost constant to a story drift angle of 1/25 rad. In other words, the connection panel did not fail in the three specimens. The deflection of beams for Specimen K2 reached 80 % of the total story drift in contrast to 60 % for Specimen K1. The difference in the beam contribution was caused by the difference in the stiffness of the columns.

Effective Width of Slab in Specimen K3 The story shear-story drift relation in the longitudinal direction for Specimen K3 is shown in Fig.8 with story shear resistances calculated with different effective slab widths; i.e., (a) the entire slab width (total width B of T-section = 2,390 mm), (b) the cooperating width specified by the AIJ Standard (B = 740 mm), and (c) no cooperating slab width (B = 200 mm). In a small story drift range, the stiffness was observed similar to the one calculated with no cooperating slab width. The resistance at a story drift angle of 1/69 rad was observed almost equal to the value calculated with the entire slab width.

The slab reinforcement in the entire slab width can contribute to the flexural resistance of the longitudinal beams even though the slab may be located only on one side of the transverse beams. The transverse beams must resist torsional moment induced by the anchoring forces of the slab reinforcement.

SHEAR STRESS LEVEL IN CONNECTION

The maximum shear stress in the connection during the uni-directional loading is normalized by the concrete compressive strength f_c' and is shown in Fig.9 for Specimens K1, K2 and K3 and for plane beam-column connection specimens J1(Ref.3) and C1(Ref.1). The effective joint area to resist shear is defined as the column depth multiplied by the average of the beam and column widths. Specimen J1, in which the maximum shear stress reached 0.25

f_c', failed in joint shear after beam flexural yielding. On the other hand, the shear stress reached as high as 0.37 f_c' and 0.35 f_c' in Specimens K1 and K3 (in the transverse direction), respectively, without failing in the connection. The orthogonal beams framing into the connection and the slabs might have confined the joint core concrete although the flexural cracks in the orthogonal beams at the column faces might remain open. The reinforcing bars in the orthogonal beams might restrain the opening of internal cracks of the joint core concrete.

The maximum shear under the bi-directional loading is summarized in Table 1. The shear under the bi-directional loading was less than 1.41 times the larger of the maximum shear forces in the two directions. This was caused by the degradation of resistance in one direction due to the bi-axial interaction of resistances.

The strains parallel to the loading direction in the joint lateral reinforcement are shown in Fig.10 for Specimen K2 at a story drift angle of 1/92 rad and for comparable plane beam-column joint specimen C1 in the input shear stress of approximately 0.18 f_c'. The strains in Specimen K2 was about half of those in Specimen C1. The width of diagonal shear cracks in the joint core must have been restrained by the beams normal to the loading direction.

CONCLUDING REMARKS

From the test results, the following conclusions were drawn;

1) Three-dimensional specimens did not fail in joint shear despite a high shear stress level in the connection, probably because the joint core was confined by the orthogonal beams and slabs.

2) The interior beam-column subassemblage with slabs, provided with good bond characterisitics along beam bars within the connection, showed a pinching behavior, which may be caused by the delay in crack closing attributable to shift in the location of the neutral axis above the beam top reinforcement under positive loading.

3) The slab width, contributing to the beam flexural resistance, spreads with beam deformation. The entire slab width needs be regarded effective at a large deformation. The edge beam, where the slab reinforcement is anchored, must be designed to resist torsional moment exerted by the tension forces of slab reinforcement in the entire width.

REFERENCES

1. Kitayama, K., K. Kurusu, S. Otani and H. Aoyama, "Behavior of Beam-Column Connections with Improved Beam Reinforcement Bond", Transaction of JCI, Vol.7, 1985, pp.551-558.
2. Paulay, T. and R. Park, "Joints in Reinforced Concrete Frames Designed for Earthquake Resistance", Research Report 84-9, Department of Civil Engineering, University of Canterbury, June, 1984.
3. Kobayashi, Y., M. Tamari, S. Otani and H. Aoyama, "Experimental Study on Reinforced Concrete Beam-Column Subassemblages(in Japanese)", Transaction of 6th JCI Annual Meeting, 1984, pp.653-656.
4. Architectural Institute of Japan, "AIJ Standard for Structural Calculation of Reinforced Concrete Structures (in Japanese)",revised in 1982.

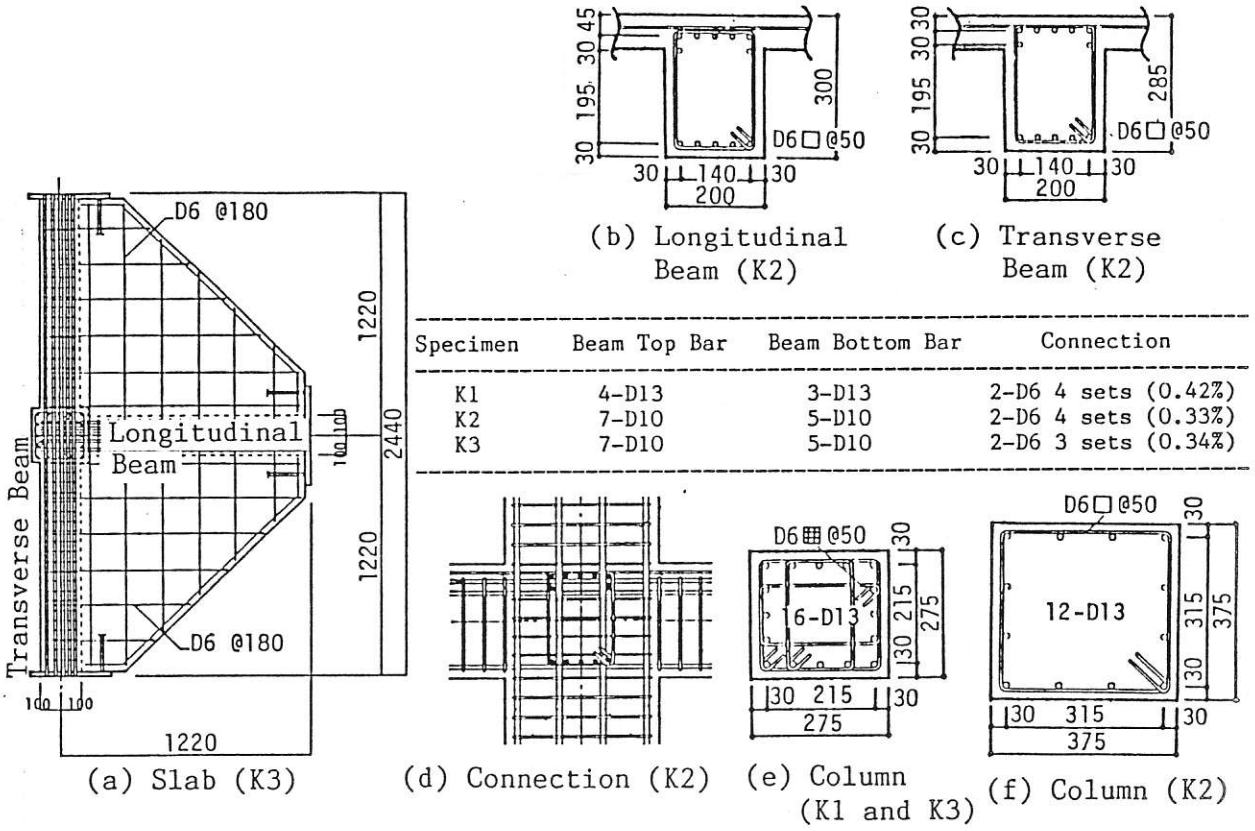

Specimen	Beam Top Bar	Beam Bottom Bar	Connection
K1	4-D13	3-D13	2-D6 4 sets (0.42%)
K2	7-D10	5-D10	2-D6 4 sets (0.33%)
K3	7-D10	5-D10	2-D6 3 sets (0.34%)

Fig.1 : Member Sections and Reinforcement Details

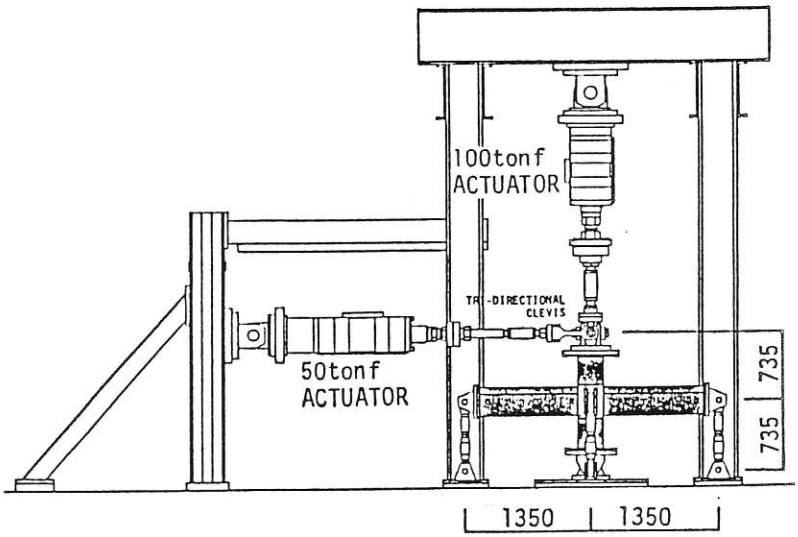

Fig.2 : Loading Apparatus

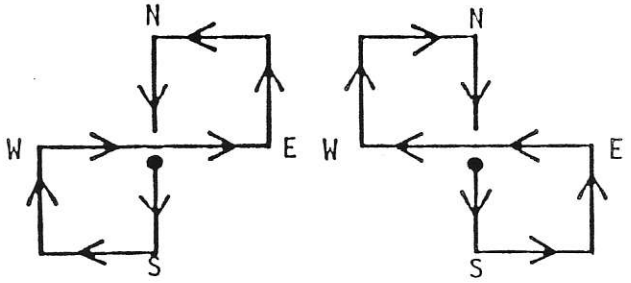

Story Drift $2\Delta_y$ Story Drift $4\Delta_y$

Fig.3 : Story Displacement Path of Loading

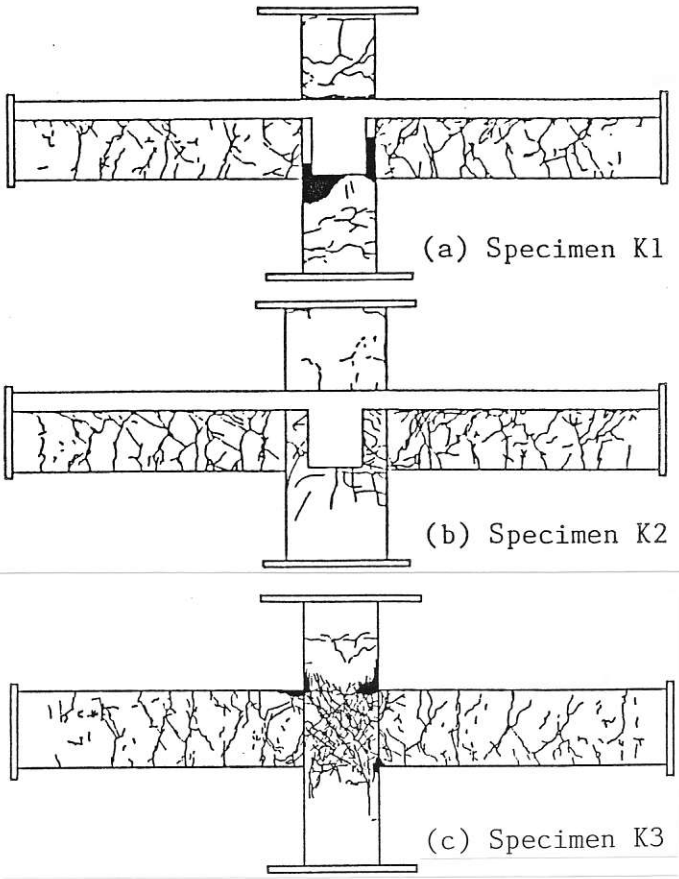

Fig.4 : Crack Patterns after Test

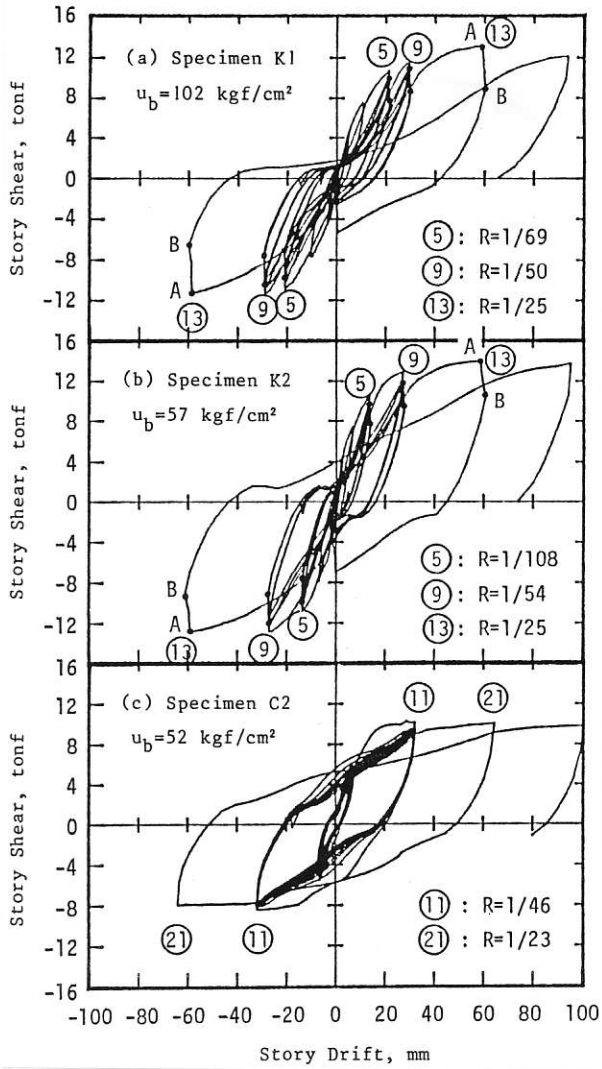

Fig.5 : Story Shear-Story Drift Relations

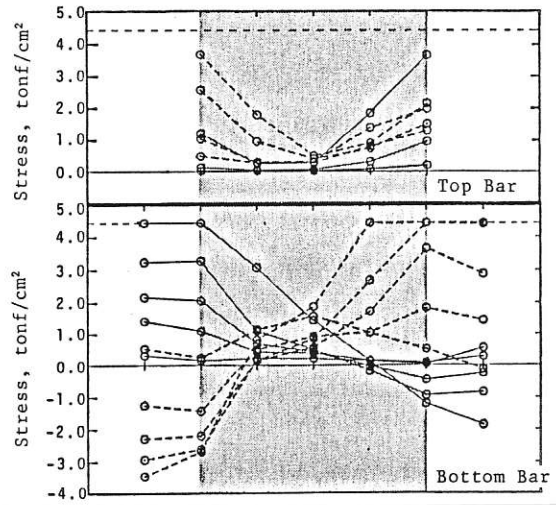

Fig.6 : Stress Distribution along Beam Bar (Specimen K2)

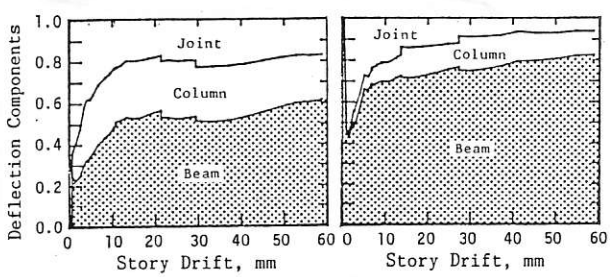

Fig.7 : Deflection Components of Story Drift

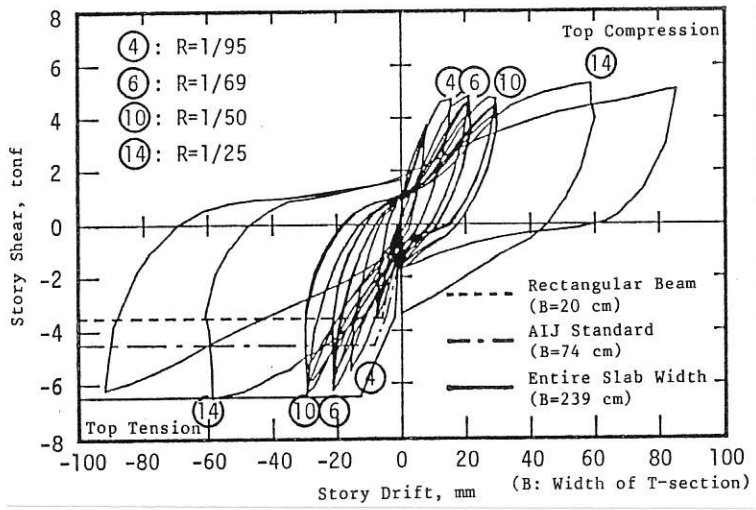

Fig.8 : Story Shear-Story Drift Relation (Specimen K3, Longitudinal Direction)

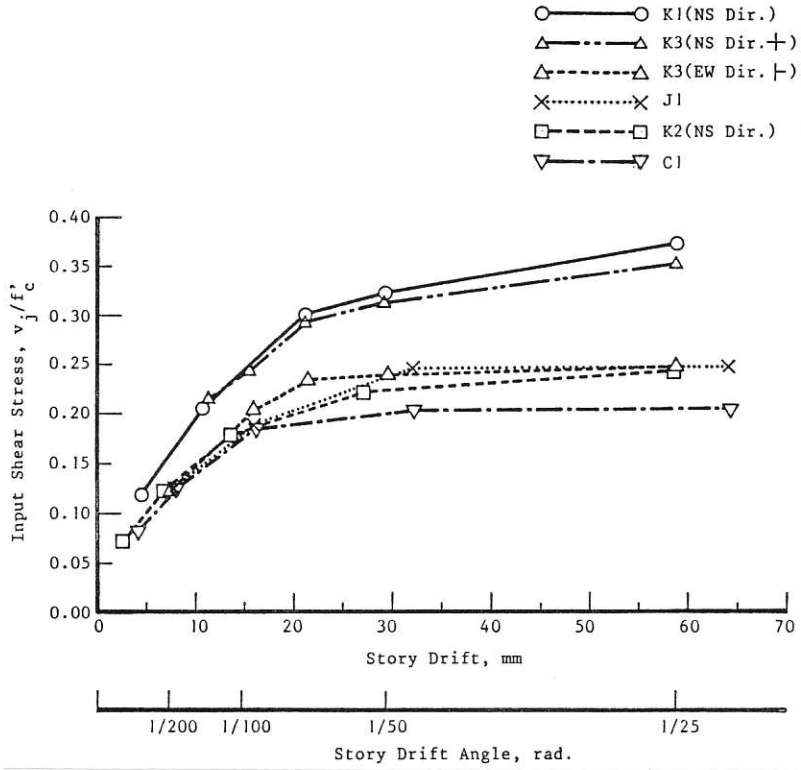

Fig.9 : Shear Stress into Connection -Story Drift Relations

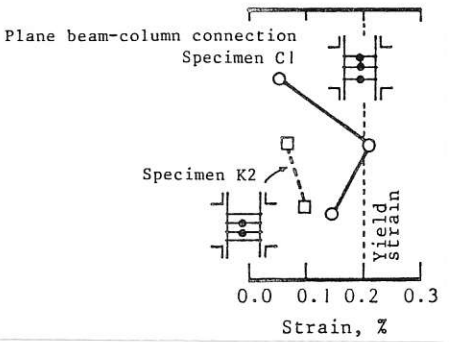

Fig.10 : Strains in Joint Lateral Reinforcement

Table 1 : Maximum Shear Force in Connection

Specimen	Input shear (Longi. Dir.) tonf(kN)	Input shear (Transv. Dir.) tonf(kN)	Resultant shear tonf(kN)	Shear stress divided by f_c'
K1	40.9(401)	52.9(519)	66.8(655) [88.3]*1	0.36
K2	50.7(497)	58.0(569)	77.1(756) [54.8]*1	0.22
K3	45.8(449)	16.6(163)	48.7(478) [64.4]*1	0.32

*1: Resultant shear stress in kgf/cm^2. The gross section of a column was used for the effective joint area to resist shear.